

# Wind turbine high-speed shaft bearings health prognosis through a spectral Kurtosis-derived indices and SVR



Lotfi Saidi<sup>a,\*</sup>, Jaouher Ben Ali<sup>a</sup>, Eric Bechhoefer<sup>b</sup>, Mohamed Benbouzid<sup>c,d</sup>

<sup>a</sup> University of Tunis, ENSIT – Laboratory of Signal Image and Energy Mastery (SIME), LR 13ES03, 1008, Tunisia

<sup>b</sup> Green Power Monitoring Systems, LLC, VT 05753, USA

<sup>c</sup> University of Brest, FRE CNRS 3744 IRDL, 29238 Brest, France

<sup>d</sup> Shanghai Maritime University, Shanghai, China

## ARTICLE INFO

### Article history:

Received 6 September 2016

Received in revised form 10 December 2016

Accepted 5 January 2017

Available online 11 January 2017

### Keywords:

High speed shaft bearing

Fault prognosis

Spectral kurtosis

Kurtogram

Support vector regression

## ABSTRACT

A significant number of failures of wind turbine drivetrains occur in the high-speed shaft bearings. In this paper, a vibration-based prognostic and health monitoring methodology for wind turbine high-speed shaft bearing (HSSB) is proposed using a spectral kurtosis (SK) data-driven approach. Indeed, time domain indices derived from SK are used and a comparative study is performed with frequently used time-domain features in the bearing degradation health assessment. The effectiveness is quantified by two measures, i.e., monotonicity and trendability. Among those features, the area under SK is utilized for the first time as a condition indicator of rolling bearing fault. A support vector regression (SVR) model was trained and tested for the prediction of the HSSB lifetime prognostics, showing the superiority of SK-derived indices of degradation assessment. We verified the potential of the prognostics method using real measured data from a drivetrain wind turbine. The experimental results show that the proposed approach can successfully detect an early failure and can better estimate the degradation trend of HSSB than traditional time-domain vibration features.

© 2017 Elsevier Ltd. All rights reserved.

## 1. Introduction

Bearings used in wind turbine generators (WTGs) are subjected to harsh environments during operation, including vibrations and shocks under varying wind speed. These loads push the bearings beyond their limits, which can explain the higher than expected failure rate [1–5].

Ambitious worldwide renewable energy targets are pushing wind energy to become a mainstream power source. Despite high wind turbine availability (>96%, depending on turbine), and a relatively low failure rate of mechanical components compared to electrical components, failures of mechanical components in drivetrains often create high repair costs and revenue loss due to long down times [1,6].

In most WTGs concepts, a gearbox is commonly used to adjust the rotor speed to the generator speed. Today, the actual service life of wind turbine gearboxes is less than the lifecycle designed of 20 years [6]. Failures can be found at several bearing locations, predominantly planet bearings, intermediate shaft and high-speed shaft bearings (HSSBs) [2] (Fig. 1).

WTG rolling element bearings (REBs) are incorporated in the support of the rotor and rotor shaft, the gearbox shafts, and the generator input shaft. The bearing arrangement depending heavily on the layout of a drivetrain. Rotor shaft bearings support the main shaft as well as the rotor blades, operating under dynamic axial and radial load conditions as well as slow speeds, approximately 20–30 rpm. The rotor blades impose cyclic loads onto the main shaft, thus causing the shaft itself to bend, resulting in misalignment within the bearings. Intermediate speed and high-speed bearings in the gearbox can also be subject to damage from these loads [2–6].

Vibration analysis is the most common condition monitoring technology used in the industry for any kind of rotating equipment and is an effective tool for the bearing fault diagnosis [1–5]. Vibration based techniques are commonly used to detect bearing faults in WTGs. In order to detect bearing faults effectively and to develop more sophisticated vibration based algorithms for fault detection, a thorough understanding of vibration signatures of bearings with faults is required. Various methods are described in the literature [1,7,14,19].

The vibration analysis methods dedicated to bearing fault diagnosis can be classified into time-domain, frequency-domain, and time-frequency based approaches [8,9]. A number of scholars have

\* Corresponding author.

E-mail address: [lotfi.saidi@esstt.rnu.tn](mailto:lotfi.saidi@esstt.rnu.tn) (L. Saidi).

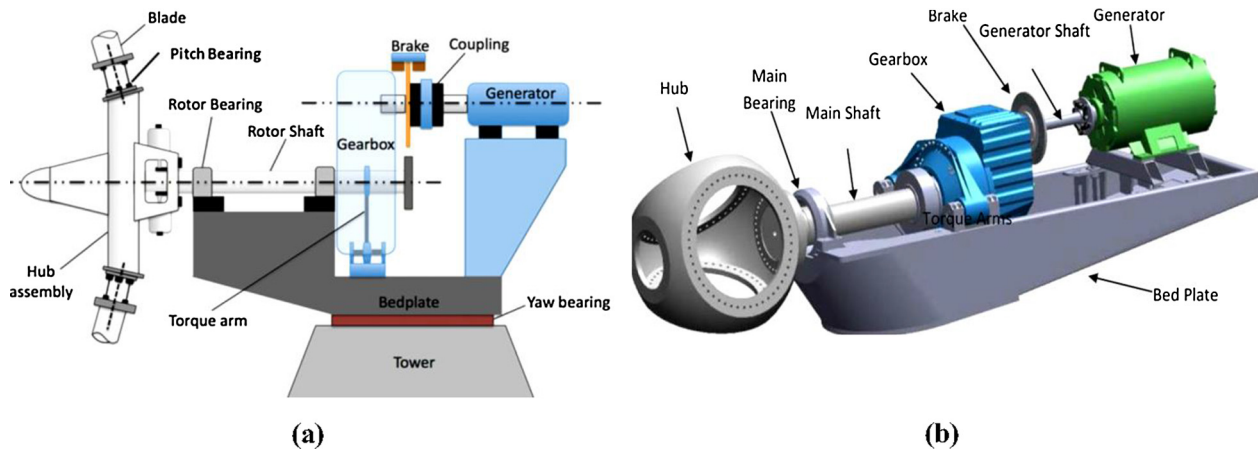


**Fig. 1.** (a) Components of the WTG including; tower; yaw system; generator; gearbox; low-speed shaft (main shaft); HSS; blades; nacelle; hub; meteorological unit (anemometry and wind vane); brake system; main bearing [2]. (b) A simplified representation of the three-bladed WTG nacelle with a zoom on its drivetrain [2].

studied the vibration signals behavior generated by REB to estimate their remaining useful life (RUL).

In [10], Soualhi et al. an approach is presented that combined the Hilbert-Huang transform, support vector machine (SVM), and support vector regression (SVR) for the monitoring of REBs. This approach indicates health, classifies the degradation severity and predicts the RUL. Experimental results show a reliable method for bearing condition monitoring.

Boškoski et al. [11], proposed an approach to estimate the RUL for REBs fault prognostics that uses Rényi entropy, Bayes' rule, and non-parametric Gaussian process models. The proposed approach was evaluated on the dataset provided for the IEEE Prognostics and Health Management (PHM) 2012 Prognostic Data Challenge.

In [12], Ben Ali et al. proposed a method based on a data-driven prognostic approach, exploring the combination of Simplified Fuzzy Adaptive Resonance Theory Map neural network and Weibull distribution. They were able to judge the health state of REBs and to estimate the RUL using these PHM tools. Experimental results showed that their proposed method could effectively predict the RUL of REBs based on vibration signals.

Detection of localized faults in planet bearings is more difficult than fixed-axis bearings because of the complicated and time-varying vibration transmission path between the fault and a measurement point on a ring gear. No published work has been found which simulates this time-varying transmission path and determines the vibration signature of a planetary drive containing a localized planet-bearing fault.

The envelope analysis, also called the high-frequency resonance technique (HFRT), is a powerful tool in these conditions [16]. It is widely used for demodulating resonances detected using the classical spectrum. But in practice, choosing a suitable resonance frequency is a challenging task.

The localization of main resonances to be a difficult task and will increase the computational time if we must analyse all resonances which can arise using the classical spectrum. Kurtosis can make this procedure less difficult; it is a scalar measurement which makes it possible to locate transients in the signal. Spectral Kurtosis (SK) is one of the new methods, that is used to locate the optimal band frequency [17,20–22].

The main objective of this paper is to investigate wind turbine HSSB degradation in run-to-failure testing using time indicators derived from SK, then estimate the RUL using SVR.

The decision whether a particular experimental run is likely to contain degradation data was based on the maximum value of the

SK for the particular measurement. The idea behind this approach is the property of the SK which states (Antoni et al., [20]) that the value of  $SK(f)$ , defined by Eq. (2), increases with the intensity of the fluctuations in the impulse amplitudes [20]. Consequently, the value of the SK can be used as an indication of the severity of the damage.

This paper is organized as follows. Section 2 introduces the WTG and its drivetrain and the bearings operation conditions and challenges. Section 3 presents a brief description of SK technique. Section 4 shows the resulting benefits by means of experimental tests using SK-derived features and RUL estimation. Finally, Section 5 concludes this paper.

## 2. Inspections of wind turbine drivetrain

### 2.1. Structure of wind turbines and bearings

Wind power generation is rapidly growing as a source of clean and green energy. Wind is available free of charge: the main costs for WTGs are construction and maintenance. The design life of wind turbines is 20-year [2–6], therefore, WTGs require periodic inspections and repairs in order to achieve this estimated 20-year lifespan. Throughout this operating period, the gearbox, bearings, blades and all other parts of each wind turbine are thoroughly inspected [23,28].

A typical three-blade horizontal axis WTG is shown in Fig. 1(a) [7]. Its internal structure and major components are illustrated in Fig. 1(b). The WTG has these major components; the nacelle is a box-shaped housing unit installed next to the turbine's blade whose rotation is powered by the wind. Inside the nacelle is a main shaft that enables the rotation of the rotor blade; a gearbox which increases the rotation speed in order to generate electric power; a generator which converts the wind power to electrical power; and a yaw system drive that changes the direction of the turbine in accordance with the direction of the wind. The wind turbine rotor is composed of the wind turbine blades, where the aerodynamic power conversion takes place, and the hub, where the blades and the low-speed shaft are attached. Furthermore, most modern wind turbine rotors are equipped with pitch servos inside the hub, that rotate the blades along their longitudinal axes to control the aerodynamic behavior of the blades [2–8].

As shown in Fig. 1(b), the nacelle of a WTG contains the power transmission system/drivetrain, the electric generator, control subsystems and some auxiliary elements such as cooling and mechanical braking systems. The drivetrain transmits the mechanical power captured by the rotor to the electric generator. It consists

of a low-speed shaft coupled to the rotating hub, a gearbox (speed multiplier) that increases the low rotational speed of the rotor to a higher speed suitable for the electric generator (typically 1:80–1:100), and a high-speed shaft (HSS) driving the electric generator. The drive train components and nacelle cover are mounted onto a bed-plate, which in turn, is positioned on top of a yaw system that is designed to automatically orient the rotor blades into the wind.

## 2.2. Bearing operating conditions and challenges

The HSS is supported by the high-speed stage bearings located on the front and back sides of the shaft, which rotates from 1500 to 1800 rpm during power generation. If there is any misalignment between the HSS and the connected generator, increased vibrations will occur and may cause damage to the bearings. The high-speed stage bearings may also be damaged by foreign matter, air or moisture contained in the lubrication oil. What is worse, due to the high-speed rotation of the high-speed stage bearings, once a bearing roller has broken, it may lead to degradation of other parts of the gearbox, resulting in a need to replace the entire gearbox [3].

Rotor shaft bearings repeat start, acceleration, deceleration and stop operations irregularly as and are exposed to the fluctuation of the load [7]. Therefore, the optimal specifications for various parameters, including bearing type, clearance, the number of bearing rollers, crowning, and the cage must be examined for each condition (minimum load, average load, maximum load).

## 3. Definition and computation method of SK

For condition monitoring of electromechanical systems, the vibration signals associated to damaged bearing typically produce an impulsive signature [21]. Detecting that impulsive signature is a challenging task since the signature could be masked by other sources of vibration (gearboxes, shafts, etc.) and noise. Techniques and filtering methods based on SK are devoted at finding the optimal frequency and bandwidth for recovering the demodulated impulsive signature that is buried in the raw vibration waveform, using the fast kurtogram (ways to compute the SK) [22–24]. A brief review of the calculation procedure and the results of this study are provided, and the interested reader is referred to the work by Antoni and Randall [21].

Kurtosis is a statistical parameter, defined as [21];

$$\text{Kurtosis} = \frac{\frac{1}{N} \sum_{i=1}^N (x_i - \bar{x})^4}{\left( \frac{1}{N} \sum_{i=1}^N (x_i - \bar{x})^2 \right)^2} \quad (1)$$

where  $x$  is the sampled time signal,  $i$  is the sample index,  $N$  is the number of samples and  $\bar{x}$  is sample mean. This normalized fourth moment is designed to reflect the “peakedness” of the signal. The SK, of a signal, is defined as the Kurtosis of its spectral components. The SK of a signal  $x(t)$  can be defined as the normalized fourth-order spectral moment [20], i.e.,

$$SK(f) = \frac{\langle |X^4(t, f)| \rangle}{\langle X^2(t, f) \rangle^2} - 2 \quad (2)$$

where  $\langle \cdot \rangle$  represents the time-frequency averaging operator,  $X^4(t, f)$  and  $X^2(t, f)$  are the fourth-order and the second-order cumulants respectively of a band-pass filtered signal of  $x(t)$  around  $f$ .

The most important properties of this definition are as follows;

- (1) The SK of a stationary process is a constant function of frequency.
- (2) The SK of a stationary Gaussian process is identical.

The SK overcomes some limits of the global kurtosis in distinguishing a high-frequency train of shocks from noise. It can be shown that the SK of a non-stationary process  $x(n)$  affected by stationary noise  $b(t)$  is

$$SK_{(x+b)}(f) = \frac{SK_x(f)}{(1 + \rho(f))^2} + \frac{\rho(f)^2 SK_b}{(1 + \rho(f))^2} \quad (3)$$

where  $f \neq 0$ ;  $\rho(f)$  is the signal-to-noise ratios (SNR) as a function of frequency. If  $b(t)$  is an additive stationary Gaussian noise independent of  $x(t)$ , then SK becomes;

$$SK_{(x+b)}(f) = \frac{SK_x(f)}{(1 + \rho(f))^2} \quad (4)$$

The aforementioned properties clarify how the SK is capable of detecting, characterizing, and locating in frequency the presence of hidden non-stationarities. Moreover, it can be found that the basic idea behind the SK is to get a quantity that can ideally take the high values when the signal is transient, and will be zero when the signal is stationary Gaussian.

SK is affected by the window length selection. In order to determine the window length of SK, Antoni [20] used the short-time Fourier transform (STFT) to compute various window lengths of SK and selected the suitable frequency band where the kurtosis value was maximized. This technique is the kurtogram concept, where a diagram displays the different values of SK calculated by using series of filter banks with various center frequency and bandwidth. The fast kurtogram was developed by Antoni to improve the

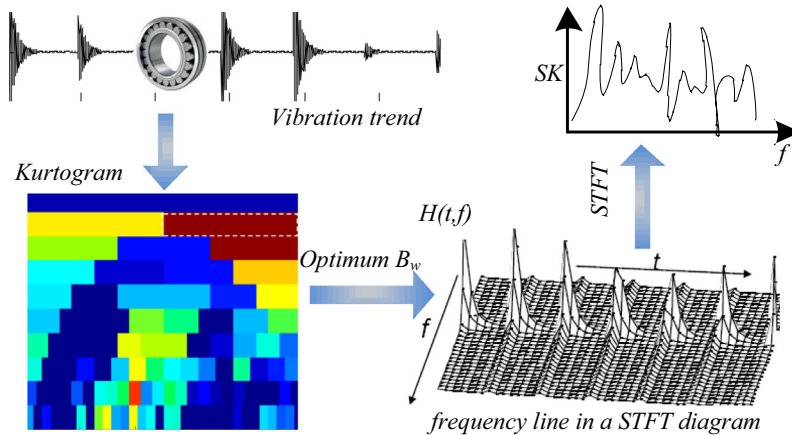


Fig. 2. Calculation of SK from the STFT; SK is an algorithm that gives an indication of how Kurtosis varies with frequency.

calculation efficiency [20–22]. It has been shown in [24,25–27] that STFT coefficients ( $t, f$ ) of each time window of the vibration signal is used to calculate the Kurtosis individually, which are then averaged to give the SK, as shown in Fig. 2. This method is similar to the Welch method for power spectral estimation. This method requires that the time window must encompass only one impulse, otherwise, the bridge between impulses will smooth Kurtosis out. However, it is very difficult to determine the time window length.



Fig. 3. Real world HSS bearing fault: At the conclusion of the data collection, an inspection of the bearing revealed a cracked inner race.

Then kurtogram was developed to overcome this problem in 2007 [21,22]. Multirate filter banks or the complex Morlet wavelets are used to decompose the vibration signal and Kurtosis is calculated based on each decomposed frequency band as a way to find the frequency band with large enough Kurtosis value. Nevertheless, the Kurtosis value depends on both central frequency " $f_c$ " and bandwidth " $B_w$ " of each frequency band, essential in determine the optimal decomposition mode [15]. In practice, many combinations of different central frequency and bandwidth have to be tried in order to find the suitable frequency band for envelope analysis, which needs considerable computation. For a comprehensive derivation of SK together with all its properties one should refer to the following Refs. [13,15,16,18].

## 4. Bearing condition monitoring

### 4.1. Experimental setup

The vibration data was collected on a commercial, 2.2 MW wind turbine (Fig. 3). Over 50 days one raw acquisition per day at high sample rate, 6 s each (sampling frequency about 100 kHz) for a real world high speed shaft bearing from a WTG provided by the Green Power Monitoring Systems in the USA. This bearing on inspection has an inner race fault. Bearings are typed SKF 32222 J2 tapered roller bearings. The TRB is 200 mm (mm) in outer diameter, with a bore of 110 mm and a total length of 56 mm. It has 20 rolling elements at a  $16^\circ$  taper angle and weighs approximately 20 lb. The

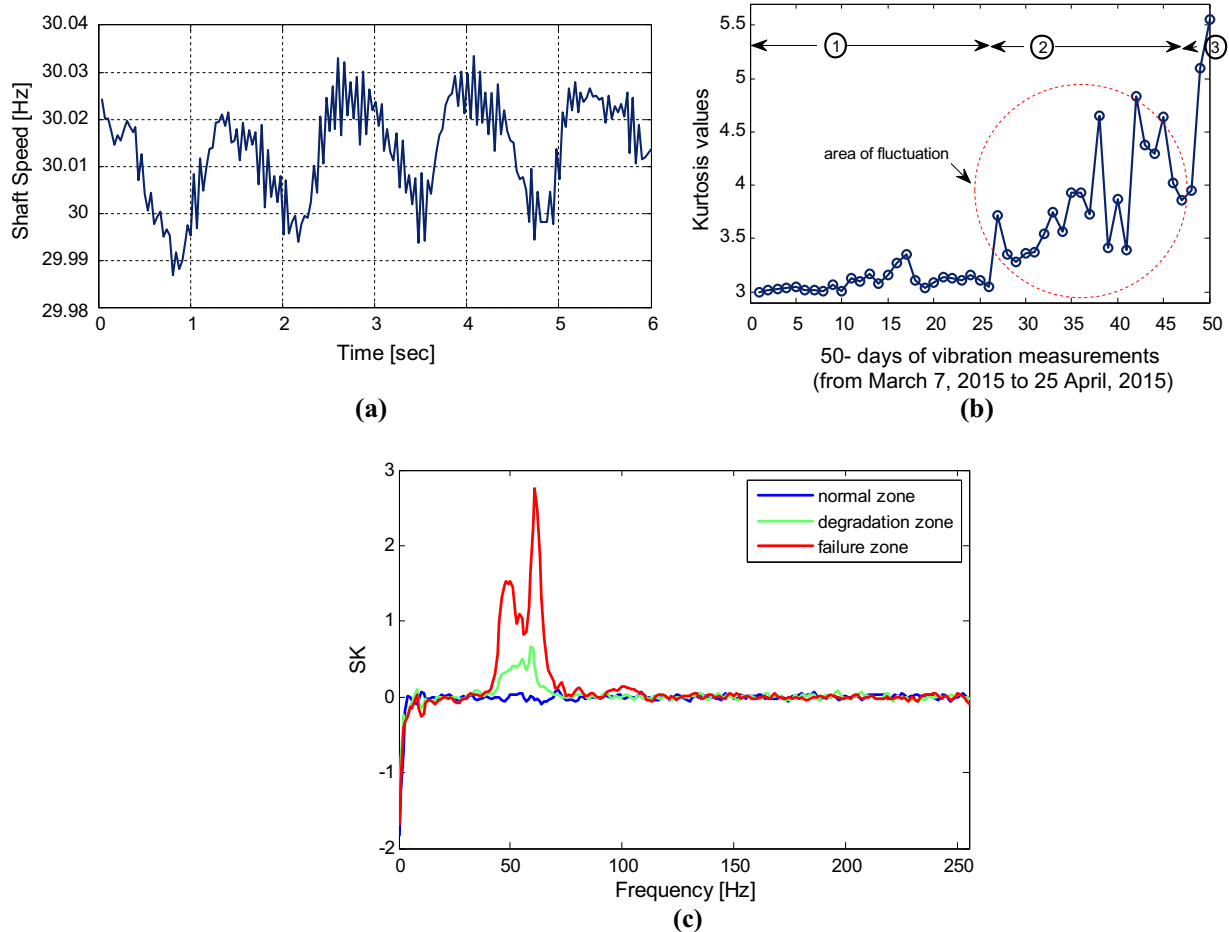


Fig. 4. (a) Variation in high speed shaft over 6 s of acquisition time. (b) Trend of the inner race fault: values of the Kurtosis for 50 measurements; (1) normal zone, (2) degradation zone and (3) failure zone, (c) SK of HSSB vibration signals for run-to-failure testing. The result tends to indicate that SK (impulsiveness) tends monotonically to failure.



bearing under test is held by the two pillow blocks. Note that the bearing under state also has a load cell to measure the force on the bearing. It's a variable speed control from 2 to 100 Hz, with a load cell to 1000 lbs. Most of the testing was done at 150 or 300 lbs. The highest test load applied was 50% of rated power to reduce the chances of a catastrophic gearbox failure.

The control of the load frame is through an MTS (Mechanical Testing Solutions) Systems-designed controller using either a handheld remote control screen (RCS) device at the load frame itself or through a software program on a dedicated computer in a separate control room. In either case, the load frame can be operated in either load or displacement control modes. In load control, a load is commanded, and the actuator displaces as much as required to achieve the desired load-up to a total of 6 in. of travel. In displacement control, a displacement is commanded, and the

actuator applies as much force as required to achieve the desired displacement-up to 110 kips.

#### 4.2. Degradation assessment

Fig. 4(a) shows the variation of a high-speed shaft on the wind turbine under test, over a 6 s acquisition. The shaft speed is approximately 30 Hz, the variation due to the effect of tower shadow and wind shear.

To track the degradation of HSSB, some of the classical extracted features such as: Kurtosis, standard deviation (std), etc. are used as indicators in this study. The values of Kurtosis for a group of 50 measurements for one particular speed (High-speed) are shown in Fig. 4(b). Under the assumption that the fault-free runs have the smallest value of Kurtosis, we can determine an area of fluctu-

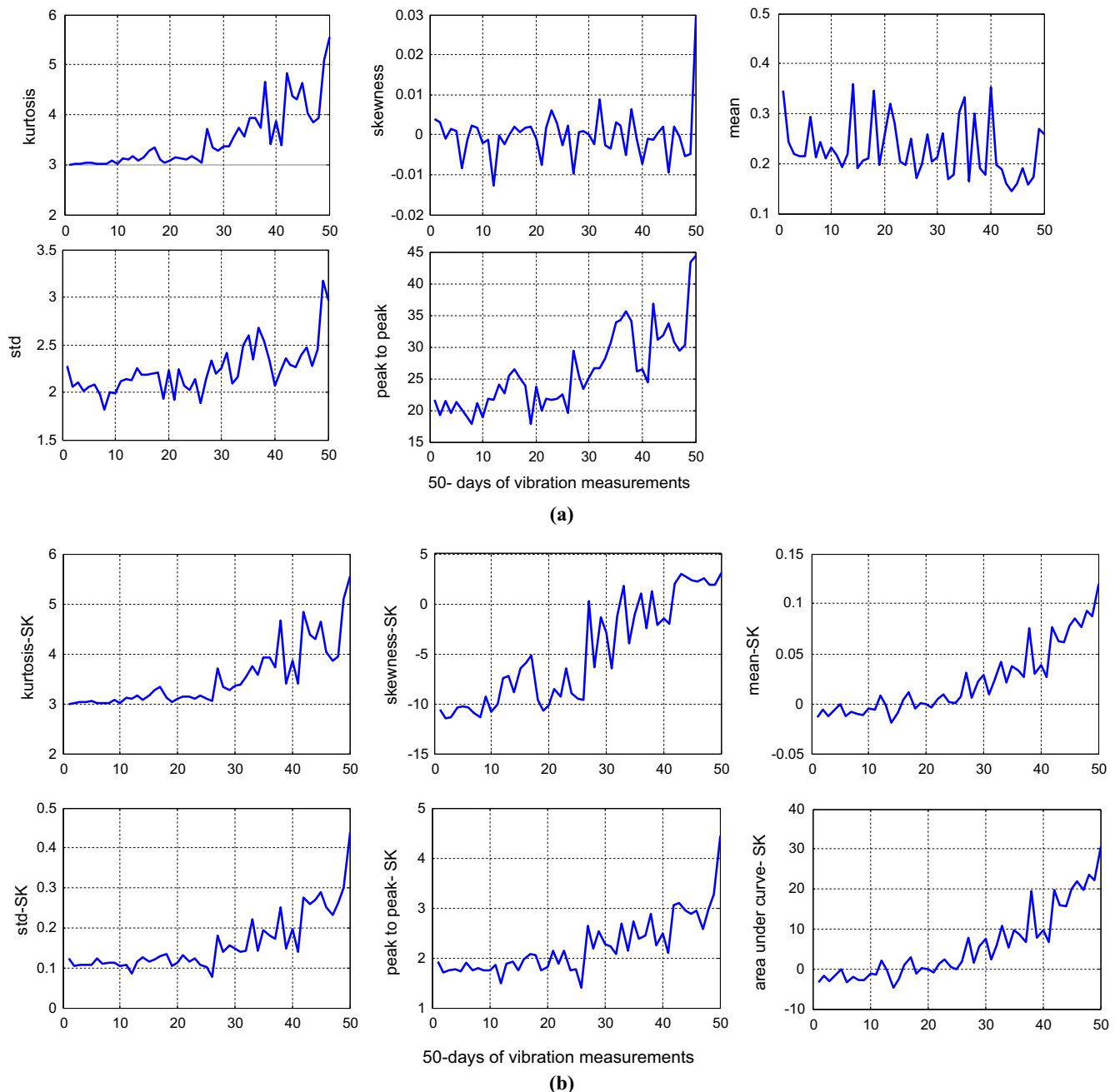


**Fig. 5.** The evolution of time-domain indices of the experimental data over the 50 days of measurements, from run- to failure. (a) Using classical indices, (b) indices derived from SK.

ation that can serve as a boundary between faulty and fault-free runs. The Kurtosis trend presented significant increases at 25th day of measurement, which can be considered to be anomaly. The procedure for selection of this area takes into account the fact that Kurtosis values for several measurements with same the kind of fault should have similar values.

From the same figure, we can also detect that the measurements with the smallest Kurtosis values are found for measurements between the 1st and 22nd day. This leads to a conclusion that the first indication of fault propagation in the HSSB configuration occurred after this interval. The Kurtosis values do not show any variation until a few days prior to failure.

SK for the experimental can be seen ground as: a normal zone (1), degradation zone (2), and failure zone (3); with the highest Kurtosis is shown in Fig. 4(b).

The inner race kurtosis indicator is trended through time, allowing the tracking of fault severity. In this case, the inner race trends upward. In this particular case, the frequency band with the highest SK can be obtained by filtering the original signal with a band-pass filter with central frequency  $f_c = 17.6$  kHz and filter bandwidth  $B_w = 1.8$  kHz.

The decision whether a particular experimental run is likely to contain degradation or not was based on the maximum value of the SK for the particular measurement. As given in Fig. 4(c), the idea behind this approach is the property of the SK which states (Antoni et al., [20]) that the value of  $SK(f)$ , defined by Eq. (2), increases with the intensity of the fluctuations in the impulse amplitudes [20]. Consequently, the value of the SK can be used as an indication of the severity of the damage. So SK values were calculated for each measurement separately.

The Kurtosis, skewness, mean, standard deviation and peak to peak indices for the HSSB were assessed and presented in Fig. 5 (a). It can be seen that the performance of time-domain indices is not satisfactory. For example, the skewness and mean oscillate around their zero amplitude values so that early HSSB degradation cannot be well-known. This will increase the difficulty of building the prognostic models. Furthermore, the time domain features are significantly divergent as the last failure values under the same loading condition, which may increase difficulty to define a failure threshold. Therefore, we must obtain features that are trendable and correlate to failure progression.

A comparative study between the traditional time domain indices and them based on SK is conducted in the next section to compare their performance in HSSB degradation trending.

#### 4.3. Degradation and indicator performance quantification

Identification of a suitable indicator simplifies the degradation assessment and prognostics. Ref. [29] proposed three metrics to quantify the suitability of the indicators: monotonicity, and trendability. They are defined as follows:

- Monotonicity describes the principal positive or negative trend of the indicator. This is an important indicator of a degradation process since the bearing fault propagation is considered to be an irreversible process. The monotonicity of a population of indicators is assumed by the average difference between the number of positive and negative growth for each path:

$$\text{Monotonicity} = \text{mean} \left( \left| \frac{\text{positive}(\text{diff}(x_i)) - \text{negative}(\text{diff}(x_i))}{n-1} \right| \right);$$

$$i = 1, 2, \dots, n$$

where  $n$  is the number of measurement time points and  $m$  is the number of systems monitored. In this study,  $m = 1$ , since 1 HSSB was tested from run-to-failure.

- Trendability specifies the degree to which the indicators of a population of systems have the same fundamental shape and can be defined by the similar function form. This will simplify the progress of a specific degradation or prognostic model. Trendability is computed by the minimum absolute correlation in a population of the indicators:

$$\text{Trendability} = \min(|\text{corrcoef}(x_i, x_j)|); i = 1, 2, \dots, m; j = 1, 2, \dots, m$$

Fig. 6 gives the performance metrics for each degradation indices. SK-derived indices avoid the effect of noise by using the optimal STFT filtering, so it is more robust than classical time-domain indices. In addition, it takes into account only the vibration generated by bearing defects: it is better correlate with the severity of bearing fault. In Fig. 6(a) and (b), classical Mean and Skewness indices are poor in monotonicity and trendability, caused by their random fluctuation and the divergence in last failure values (Fig. 5(a)). In addition, Mean and Skewness measure the whole vibration level of a signal and tend to be buried due to gear-box noise. At the early stage of HSSB faults, the vibration of bearing fault has slight effect on the whole vibration level of the whole WTG drivetrain system. As a result, Mean and Skewness may be not sensitive to incipient bearing degradation. Kurtosis and Peak to peak are sensitive to the impulsive components in the signal, and they

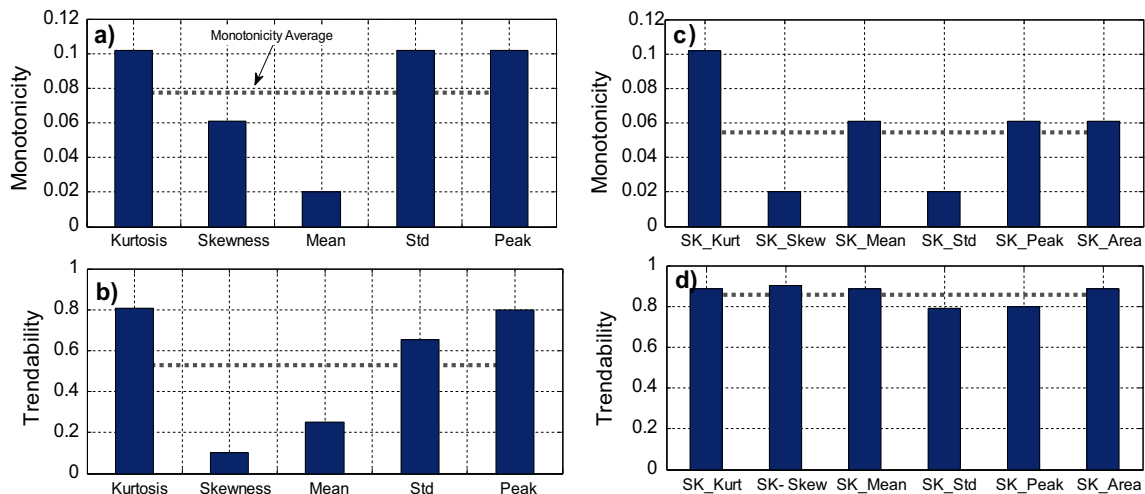


Fig. 6. Indices performance metrics: (a), (c) Monotonicity and (b), (d) trendability for classical indices and them derived from SK, respectively.

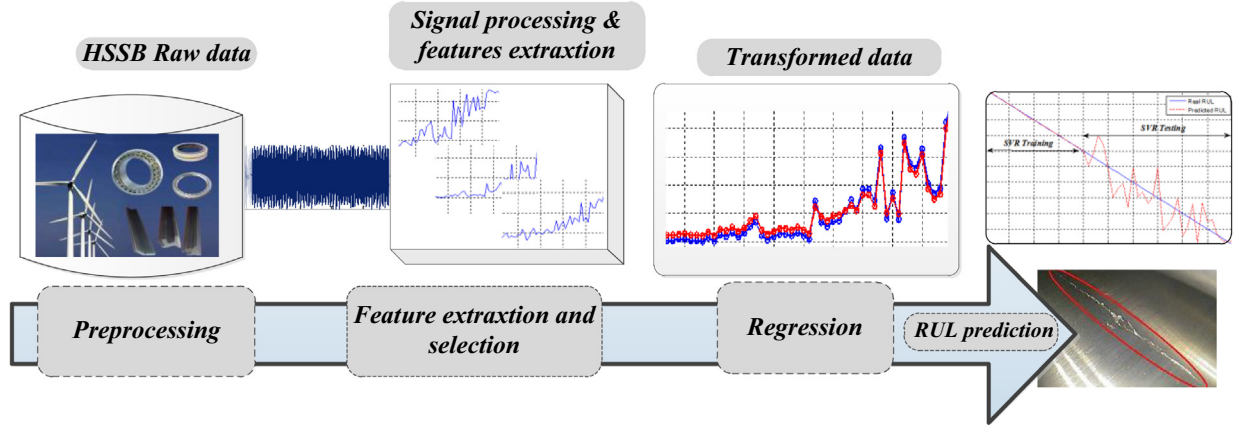


Fig. 7. A flow chart depicting the SVR regression and RUL prediction scheme.

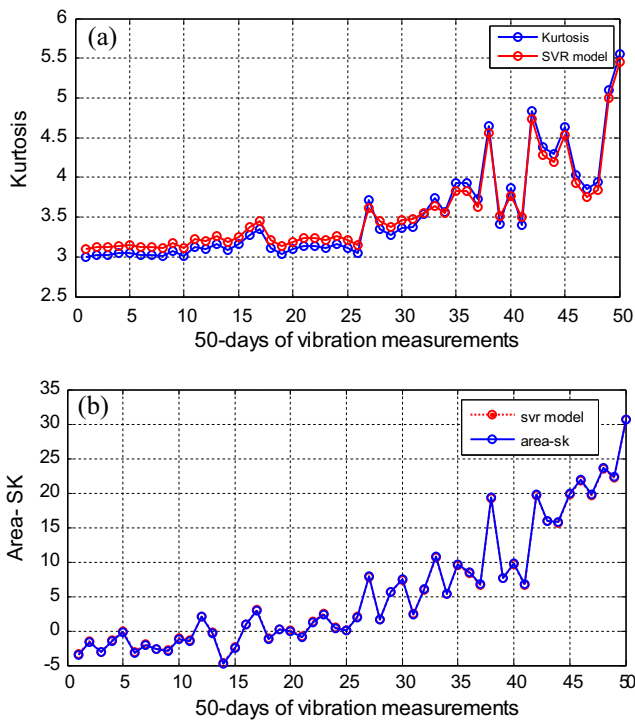


Fig. 8. (a) HSSB degradation evolution result obtained from: (a) traditional Kurtosis, (b) area under SK.

have the ability to identify early bearing degradation. The Kurtosis and Peak to peak of the HSSB indicate growing trends in the early stage of the fault process (Fig. 5(a) and (b)), indicating the early degradation of the bearing. As a result, the comparative study shows that the SK-derived indices are more powerful than classical time-domain indices. It not only can detect an early fault of HSSB, but also offer improved degradation trending than time-domain indices.

In the next section, a data-driven prognostic methodology is proposed based on SVR for the step by step prediction of the RUL of HSSB. The RUL prognosis scheme is developed and tested on a real WTG dataset provided by the Green Power Monitoring Systems in the USA. The model is trained and calibrated off-line, utilizing information from the past lifelong histories, and then tested in unseen data, which are those data that do not participate in the training phase.

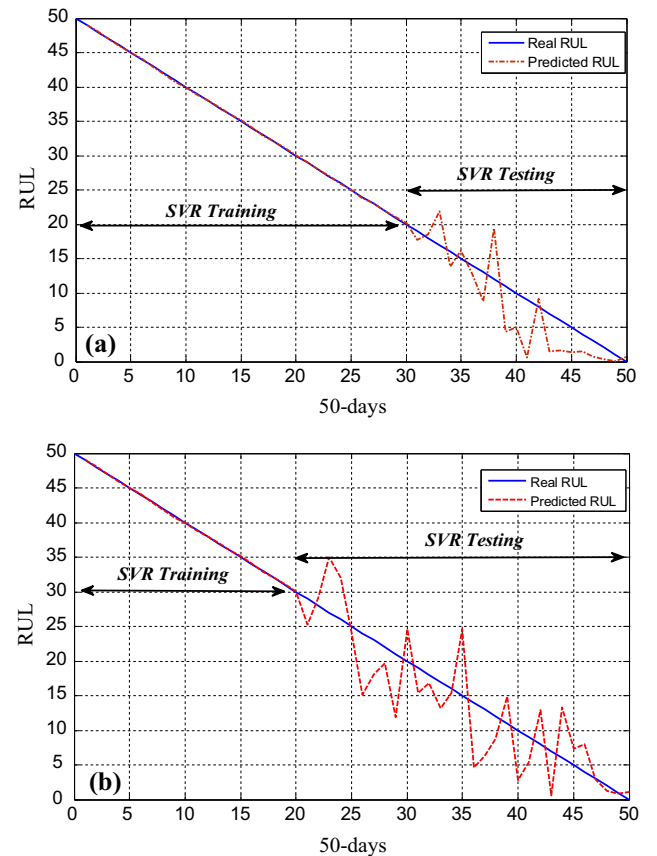


Fig. 9. Predicted RUL of a bearing degraded using SVR model obtained from: (a) 60% of training and 40% of testing data, (b) 40% of training and 60% of testing data.

#### 4.4. RUL estimation based on SVR

By using the historical run-to-failure vibration data analysis and time domain indices given in section 4.2, we can build the RUL prediction models for the degradation state and the failure state. The approach used to implement RUL prediction modelling is the SVR (Fig. 7). SVR is a powerful function approximation technique based on statistical learning theory. In other words, a regression method is an algorithm to estimate a relationship between the system input and output from the samples or training data. It is known that the estimation with the SVR is very effective for power system applications [30]. For more information about SVR, the readers can refer to [30].

Observing the resulting trends of the predicted RUL (Fig. 8 (a) and (b)), it is evident that the proposed methodology follows satisfactorily the degradation trend of the test-set HSSBs. Fig. 8(a) depicts the predicted RUL plotted in the same graph with the classical Kurtosis. It shows that the predictions initially overestimate the RUL; as the end-of-life approaches, the prediction tends to reach the actual remaining life. RUL prediction in Fig. 8(b) based on Area under SK is, from an engineering point-of-view, better estimator of RUL than classical Kurtosis.

Fig. 9 shows the predicted RUL of a bearing degraded using area under SK index obtained from: 60% of training and 40% of testing data (Fig. 9(a)), and 40% of training and 60% of testing data (Fig. 9 (b)). Although the predicted RUL curve can basically track the changing trend of the real RUL curve, there exists large fluctuation in the curve, resulting in large prediction error (Fig. 9(b)) due to the 40% of training data vs. 60% of testing data. At last, the SVR model based on area under SK index proposed in this paper is utilized for RUL has returned significantly smaller prediction error and the results are shown in Fig. 9(a) with 60% of training data.

The results demonstrate that the SVR model based on area under SK is able to estimate RUL precisely.

## 5. Conclusion

This paper deals with a health monitoring approach for WTG HSSBs. SK-derived features based methods were presented to extract the bearing characteristic vibration from the raw vibration signal. Health indices were calculated to assess the degradation severity of HSSB.

It was demonstrated that SK-derived features can provide an early warning of bearing defects and facilitates evaluating the bearing degradation. Comparative studies were conducted to compare the efficiency of these features and classical time-domain indices in the early stage of defect detection and degradation trending. It was found that Mean and Skewness failed to identify early faults since they measure the whole vibration level of the signal and are sensitive to noise effect. Kurtosis and Peak to Peak were able to detect early faults.

The achieved results indicate that the SK is still evolving and has been used successfully in fault diagnosis of the HSSBs in WTG.

Additionally, using the historical run-to-failure vibration data and time domain indices, these results were extended to RUL estimation of the HSSB, based on SVR, showing the superiority of the SK-derived features.

## References

- [1] Yang W, Tavner PJ, Wilkinson MR. Condition monitoring and fault diagnosis of a wind turbine synchronous generator drive train. *IET Renew Power Gener* 2009;3(1):1–11.
- [2] McDade M, Munch K. Gearbox reliability collaborative: gearbox inspection metadata. NREL/TP-500-49133 2010.
- [3] Amirat Y, Benbouzid MEH, Al-Ahmar E, Bensaker B, Turri S. A brief status on condition monitoring and fault diagnosis in wind energy conversion systems. *Renew Sustain Energy Rev* 2009;3(9):2629–36.
- [4] Chen B, Matthews P-C, Tavner P-J. Automated on-line fault prognosis for wind turbine pitch systems using supervisory control and data acquisition. *IET Renew Power Gener* 2015;9(5):503–13.
- [5] Oyague F. Progressive dynamical drive train modeling as part of NREL gearbox reliability collaborative: preprint. NREL Report. No. CP-500-43473. Golden, CO: NREL; 2008. p. 16.
- [6] Lacava W, Xing Y, Marks C, Guo Y, Moan T. Three-dimensional bearing load share behaviour in the planetary stage of a wind turbine gearbox. *IET Renew Power Gener* 2013;7(4):359–69.
- [7] Yagi S, Ninoyu N. Technical trends in wind turbine bearings. Osaka, Japan: NTN Corporation; 2008 [Technical Report Review, 76].
- [8] Bechhoefer E, Menon P, Kingsley M. Bearing envelope analysis window selection: using spectral kurtosis techniques. In: *Proceedings of the 2011 IEEE international conference on prognostics and health management*. p. 6.
- [9] McMillan D, Ault GW. Condition monitoring benefit for onshore wind turbines: sensitivity to operational parameters. *IET Renew Power Gener* 2008;2(1):60–72.
- [10] Soualhi A. Bearing health monitoring based on hilbert-huang transform, support vector machine, and regression. *IEEE Trans Instrum Meas* 2014;64(1):52–62.
- [11] Bošković P, Gašperina M, Petelina D, Juričića D. Bearing fault prognostics using Rényi entropy based features and Gaussian process models. *Mech Syst Signal Process* 2015;52–53:327–37.
- [12] Ben Ali J, Chebel-Morellob B, Saidi L, Malinowski S, Fnaiech F. Accurate bearing remaining useful life prediction based on Weibull distribution and artificial neural network. *Mech Syst Signal Process* 2015;56–57:150–72.
- [13] Saidi L, Ben Ali J, Fnaiech F. Bi-spectrum based-EMD applied to the non-stationary vibration signals for bearing faults diagnosis. *ISA Trans* 2014;53(15):1650–60.
- [14] Saidi L, Fnaiech F. Bearing defects decision making using higher order spectra features and support vector machines. In: *The 14th international conference on sciences and techniques of automatic control & computer engineering (STA)*. p. 419–24.
- [15] Saidi L, Ben Ali J, Fnaiech F. Application of higher order statistics and support vector machines for bearing faults classification. *ISA Trans* 2015;54:193–206.
- [16] Barszcz T, Jabłoński A. A novel method for the optimal band selection for vibration signal demodulation and comparison with the Kurtogram. *Mech Syst Signal Process* 2011;25(1):431–51.
- [17] Sawalhi N, Randall RB. Spectral kurtosis optimization for rolling element bearings. In: *Proceedings of the 8th international symposium on signal processing and its applications* [p. 839–842].
- [18] Saidi L, Ben Ali J, Bechhoefer E, Benbouzid M. The use of SESK as a trend parameter for localized bearing fault diagnosis in induction machines. *ISA Trans* 2016;63:436–47.
- [19] Ben Ali J, Fnaiech N, Saidi L, Chebel-Morellob B, Fnaiech F. Application of empirical mode decomposition and artificial neural network for automatic bearing fault diagnosis based on vibration signals. *Appl Acoust* 2015;89:16–27.
- [20] Antoni J. The spectral kurtosis: a useful tool for characterizing non-stationary signals. *Mech Syst Signal Process* 2006;20:282–307.
- [21] Antoni J, Randall RB. The spectral kurtosis: application to the vibratory surveillance and diagnostics of rotating machines. *Mech Syst Signal Process* 2006;20:308–31.
- [22] Antoni J. Fast computation of the Kurtogram for the detection of transient faults. *Mech Syst Signal Process* 2007;21:108–24.
- [23] International Organization for Standardization. Wind turbines – Part 4: Standard for Design and Specification of Gearboxes. ISO/IEC 81400-4:2005. Geneva, Switzerland: ISO, February 2005; 2005.
- [24] Obeid Z, Picot A, Poignant S, Regnier J, Darnis O, Maussion P. Experimental comparison between diagnostic indicators for bearing fault detection in synchronous machine by spectral Kurtosis and energy analysis. In: *IECON2012 – 38th annual conference of IEEE INDUSTRIAL ELECTRONICS (IECON2012)*; 2012. p. 3901–06.
- [25] Immoivilli F, Cocconcelli M, Bellini A, Rubini R. Detection of generalized-roughness bearing fault by spectral-Kurtosis energy of vibration or current signals. *IEEE Trans Ind Electron* 2009;56(11):4710–7.
- [26] Leite VCMN, da Silva JGB, Veloso GFC, da Silva LEB, Torres G, Bonaldi EL, et al. Detection of localized bearing faults in induction machines by Spectral Kurtosis and envelope analysis of stator current. *IEEE Trans Ind Electron* 2015; 62: 1855–65.
- [27] Fournier E, Picot A, Regnier J, Yamdeu, MT, Andrejak JM, Maussion P. On the use of Spectral Kurtosis for diagnosis of electrical machines. In: *9th IEEE international symposium on diagnostics for electric machines, power electronics and drives*, 2013; 2011. p. 77–84.
- [28] Amirat Y, Choqueuse V, Benbouzid MEH. EEMD-based wind turbine bearing failure detection using the generator stator current homopolar component. *Mech Syst Signal Process* 2013;41(1–2):667–78.
- [29] Coble JB. Merging data sources to predict remaining useful life-an automated method to identify prognostic parameters. Knoxville: The University of Tennessee; 2010 [Doctoral dissertation].
- [30] Soualhi A, Medjaher K, Zerhouni N. Bearing health monitoring based on hilbert-huang transform, support vector machine, and regression. *IEEE Trans Instrum Meas* 2014;64(1):52–62.